ORIGINAL ARTICLE

Microfabrication of Sm2Co17 micromagnets for MEMS and micromotors using ultrashort pulsed hydro laser micromilling process

Gabriel Villalba-Alumbreros[1] · Jimena Soler-Morala[2] · Alberto Bollero[2,3] · Alexander Kanitz[4] · Jan Hoppius[4] · Ignacio Valiente-Blanco[1] · Efren Diez-Jimenez[1]

Abstract

Micromagnets have wide applications in MEMS and micromotors but there are still miniaturization limitations in current microfabrication processes for permanent magnets. A novel damage-free ultrashort pulsed laser machining process to manufacture complex shapes of Sm2Co17 micromagnets is proposed in this work. Laser process permits to further miniaturize the size of the resulting micromagnets achieving very small micromagnets. This can be achieved as micromagnets are submerged in a refrigerant fluid which is especially beneficial for magnets that are materials very sensitive to high temperature. The heat effect of laser cutting on the hard magnetic materials is drastically reduced thanks to the fluid. The detailed description of the manufacturing process is hereby presented. Results of several machining processes like milling and cutting and the magnetic characterization of the resulting micromagnets are shown. Complex segment shapes, with 65-µm thickness made in high-quality Sm2Co17 material, with good accuracy are achieved. It is demonstrated that no permanent degradation of the magnetic properties appears after laser machining.

Keywords Magnetic characterization · Micromagnets · Laser manufacturing · Micromachining

1 Introduction

Permanent magnets made of NdFeB and SmCo can reach high magnetic products, high remanence, and high coercitivity. Theses magnets are used in plenty of industrial applications: electric machines [1], mechanical damping [2, 3], braking [4], or contactless transmission [5] systems. In MEMS (Micro-ElectroMechanical Systems) [6–8] and micromachines [9–12], high-quality magnets of NdFeB and SmCo in micrometric size are required. Small micromagnets have been used in several small applications such as sensors [13], actuators [14–16], robotic manipulators [17, 18], and medical devices [19], in particular, actuators [20, 21] and wireless intrabody power transmission systems [22]. Not only small magnets are used, structures of magnets with micrometric features, specific geometries, or magnetic multipole pattern distributions [23] are also required in MEMS applications [24]. The combined use of permanent magnets, micrometric high-quality ferromagnetic parts [25], and microinductors [26, 27] makes possible to achieve high specific power, torque, and force in MEMS devices.

Manufacturing of hard permanent micromagnets for micrometric scales can be approached by three ways [28]. First method is used to obtain bonded micromagnets by using composite and molds. Using magnetic powder and organic polymers, a nanocomposite of bonded magnet can be created. Through a UV-LIGA process, the mold can be created on a photo-patternable flexible polymer [29]. Afterwards, the composite fills the mold, the excess is scraped off, and then the mold is removed [30]. This process offers

✉ Gabriel Villalba-Alumbreros
  gabriel.villalba@uah.es

  Efren Diez-Jimenez
  efren.diez@uah.es

[1] Mechanical Engineering Area, Signal Theory and Communications Department, Universidad de Alcalá, 28801 Madrid, Spain

[2] Group of Permanent Magnets and Applications, IMDEA Nanoscience, 28049 Madrid, Spain

[3] R/ATM4, Robert Bosch GmbH, Renningen, Germany

[4] Lidrotec GmbH, Universitätsstraße 150, 44801 Bochum, Germany

magnets in a variety of small shapes, but the magnetic properties of the results magnets are much lower than a bulk sintered magnet. A second way for obtaining micromagnets is by deposition techniques. A layer of magnetic material with adhesive and antioxidation doping is deposited using techniques such as magnetron sputtering or triode sputtering over a silicon substrate [31, 32]. Good magnetic properties and accurate shapes are achieved using these procedures. Nevertheless, extracting the individual magnets from substrates is not easy. The whole process requires long time processing, and it is costly. A third way to obtain individual micromagnets with high magnetic quality is machining sintered bulk magnets. Smallest magnets using mechanical machining methods have between 110 and 250 μm as characteristic length. Further miniaturization is not possible as magnets are brittle materials, which is an important pitfall that makes difficult to manufacture smaller volume parts and intricate shapes [33]. Therefore, alternative methods for micromagnets manufacturing should still be explored.

Ultrashort pulsed laser machining has been widely used in recent years to perform machining processes of micrometric structures and shapes in different materials like ceramics, metals, and polymers [34]. Pulsed laser machining has been applied in several microfabrication processes: drilling [35], milling [36], grooving [37], and cutting free microparts [38]. Laser machining is also a promising method to machine bulk magnets without exerting mechanical forces. As there are no mechanical forces, sample attachments can be easily done, preventing damages during part releasing process after machining. Some interesting works have demonstrated that is small sizes. For example, a Halbach cylinder with an 8-mm outer diameter and 2-mm inner diameter assembled from individual parts has been achieved using laser pulsed techniques [39]. In addition, small Sm_2Co_{17} magnets of 0.1 × 0.3 × 2 mm dimensions have been also obtained by laser machining [40]. Those previous works show excellent results on the use of pulsed laser machining applied to permanent magnet microfabrication.

In this paper, we demonstrate a step forward in miniaturization of permanent magnet microfabrication by using a special ultrashort pulsed hydro laser machining process. This process permits to cut the microparts accurately while having the parts cooled down by using refrigerant fluid [41, 42]. This process is especially beneficial when processing hard magnetic materials as excessive temperatures can lead to irreversible damage in the material structure, partially or completely losing their magnetic properties. During the cutting processes, liquids in the laser processing zone are used, which greatly cool the workpiece and remove ablation products such as particles [43]. As a result, the processing speed can be increased while maintaining high precision and achieving significantly cleaner surfaces [44]. The use of liquid has four decisive advantages compared to processing

in gas atmospheres: cooling, rinsing, chemical protection, and safety [45]. The cooling process during cutting works very efficiently since the heat transfer from the workpiece to the liquid is much greater than with gases [46]. Higher repetition rates and pulse energies can be used for the machining, therefore allowing a high process speed. In addition, the fluid carries away the removed microparticles and nanoparticles and therefore cannot attach to the surface. Chemical interactions between the material and the atmosphere are also completely avoided, preventing from oxidations. To sum up, the advantages of ultrashort pulsed hydro laser machining process are as follows: contactless machining, no need of sample strong gripping, high quality, burr-free and sharp cutting edges with high precision, free from surface contamination, minimum heat input, machining of heat sensitive materials. This process is extremely versatile as it can perform cutting, drilling, structuring, and functionalizing in one single process.

In this work, we demonstrate that using ultrashort pulsed hydro laser machining process for permanent magnets microfabrication permits to obtain micromagnets smaller than previous micrometric ones while preserving good magnetic properties. We present the target design, and the manufacturing process steps are detailed. Geometrical results of complex machined micromagnets and magnetic characterization of the micromagnets made in Sm_2Co_{17} are shown.

2 Materials and methods

The departure raw material selected for the micromagnet is Sm_2Co_{17}, discarding NdFeB. NdFeB magnets get oxidized and deteriorated if the protecting coating is removed during machining. Material coating thickness is very significant in micrometric size and most of conventional coatings for magnets like nickel, gold, or aluminum present typical thickness in the range of 20–40 μm. Therefore, coating would imply that a large portion of the magnet is not hard magnetic, reducing the final part magnetic quality. On the other hand, Sm_2Co_{17} does not required a coating; thus, there will be more portion of hard magnetic material. In addition, NdFeB is much more susceptible to high temperatures (Curie temperature of $Nd_2Fe_{14}B$ is 585 K vs 1093 K for Sm_2Co_{17}). Hence, Sm_2Co_{17} seems a more reliable magnetic material compatible with the presented method while having high magnetic properties. In terms of magnetic properties, the machined micromagnet should have as closest as possible similar values as the original magnet, once magnetized. If not, this will mean that there is a heat affected zone on the material where the structure is damaged and thus, an optimum magnetic performance will not be achieved in a final application device.

Fig. 1 Target magnet micro-segment geometry (right) and bulk raw initial magnet (left). Dimensions in millimeters
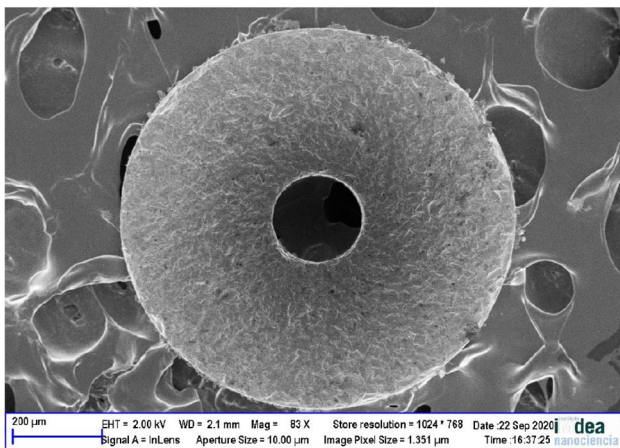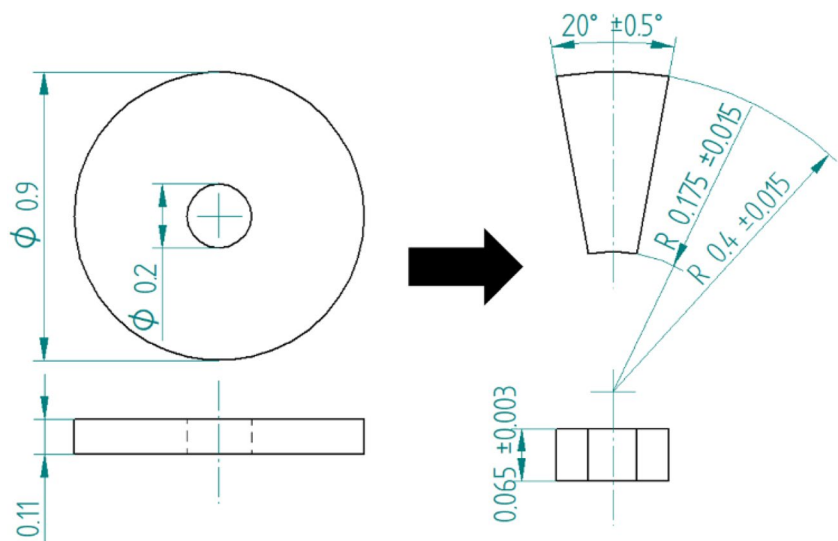

Fig. 2 SEM picture of initial Sm_2Co_{17} bulk raw material piece

The targeted geometry in this study is the microsegment-shaped shown in Fig. 1. This is a typical shape needed, for example, in axial flux electric machines where individual magnets are used. The larger radius length of the segment is about 0.139 mm and shorter radius length size is 0.061 mm. Thickness specification is 0.065 mm. The volume of the segment is, therefore, 1.443×10^{-6} cm^3 and the mass of 0.012 mg. Such a small micromagnet has never been manufactured. To create this microsegment, the departure raw bulk material is a disk of 0.9-mm diameter and 0.110-mm thick (grinded machined), as depicted in Fig. 1. 0.110 mm is the thinnest thickness that can be reached using conventional mechanical techniques. This raw part is made in Sm_2Co_{17} (Recoma35E from Arnolds magnetics) with 1.19 T of remanence and a coercivity of 880 kA/m. A SEM picture of the initial raw bulk material is shown in Fig. 2.

The micromagnets are manufactured using ultrashort pulsed hydro laser micromilling process. The laser milling system uses a commercial laser source (TRUMPF TrueMicro 2030), operating at a wavelength of 1030 nm, with a pulse width of 400 fs, a maximum pulse energy of 100 µJ, and a power of 20 W with liquid cooled part chuck, as shown in Fig. 3. Cutting speed is set 30 µm/s.

Water has been used as fluid. The height of the water layer is a few mm, typically 10 mm and was chosen following recommendations published at [47]. Focus lens distance and height of liquid shall be in good agreement to focalize the laser beam spot. The water is at room temperature. Moreover, it is important that the water cools within nanoseconds as described and shown experimentally at [43, 48].

The laser milling system includes the laser source, mirrors, shutter, aperture, electronic laser power attenuator, a high precision galvanometer scanner, focusing lens, and high-precision *XYZ* linear stages. The beam spot, with a radius of about 8 µm, was formed by the focusing lens of 70 mm. The high-precision linear stages and galvanometer scanner can accurately move in *X*, *Y*, and *Z* directions with 0.1-µm position accuracy.

The main difficulty to face in the process is machining this size micropart without breaking or damaging the material, moreover, considering the fragility of the magnets. Good quality of both machined faces is a goal to achieve. No debris, fractures, or burr are required features too in the microsegments as surface quality and accuracy in dimensions are fundamental parameters in further integration and assembling processes.

The machining process is depicted in Fig. 4 comprising three steps. First step (A) aims to reduce the thickness of the raw material from 110 to 65 µm by laser surface milling. A next rinsing step (B) is required to remove any

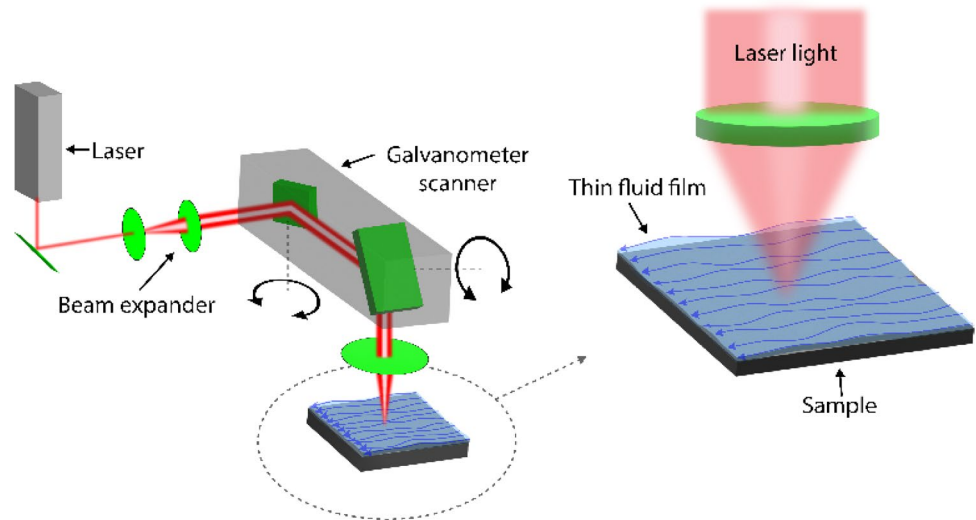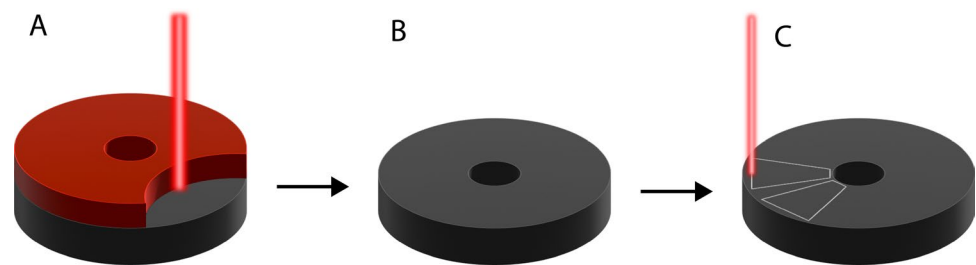**Fig. 3** Ultrashort pulsed hydro laser micromilling schematic description

Fig. 4 Machining process: **(A)** surface milling, **(B)** rinsing, **(C)** cutting of microsegments

remaining particles from the disk with the target thickness. Last step (C) is the accurate cutting the microsegments by application of an automatic grooving process.

3 Results and discussions

3.1 Manufacturing results

From a full raw disk, eight machined microsegments were laser-cut without breaking the extra raw material, as shown in Fig. 5. This result indicates that Sm_2Co_{17} can be machined with a good chip separation and without fractures. The cut groove width is measured in 15 ± 5 μm. After completion of the machining process, the raw material waste was easily removed from the final object, making possible to retrieve the eight microsegments in a clean and easy manner (see Fig. 5 and Fig. 6).

Figure 7 shows optical microscope images for two selected micromagnets separated from the initial disk magnet. They both show good-segmented shape in agreement with the design specifications. Lateral walls are almost perfectly straight, with a degree of more than 89° with respect to the horizontal plane, as shown in Fig. 7. Small curvature radii, < 10 μm, appear in the edges of the cuts.

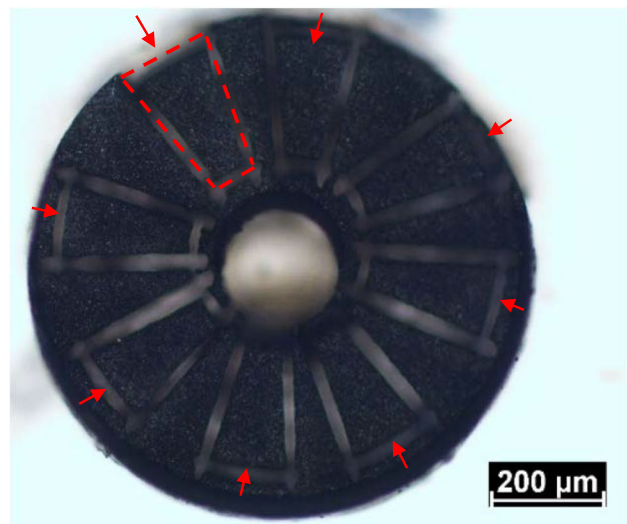**Fig. 5** Eight machined micromagnets (see red arrows) from the Sm2Co17 initial raw material disk

Different micromagnet samples have been studied to characterize the geometric parameters. A Digital microscope Olympus DSX 1000 with 3D profilometry capacity has been used. A 3D reconstruction of a machined sample is shown in
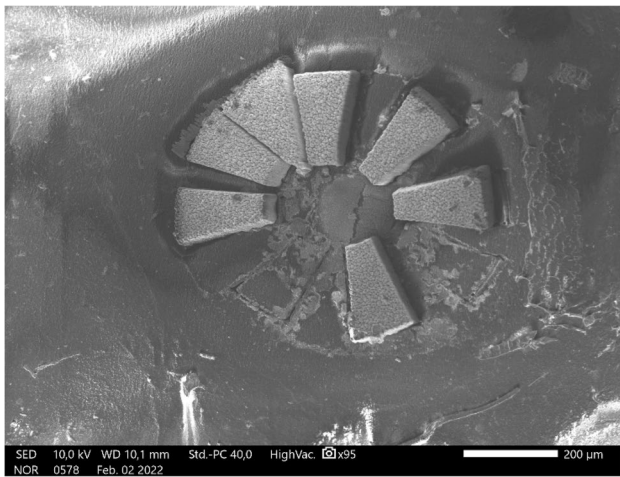
Fig. 6 SEM image of six Sm2Co17 micromagnets after removal two of them for characterization and removal of the raw material
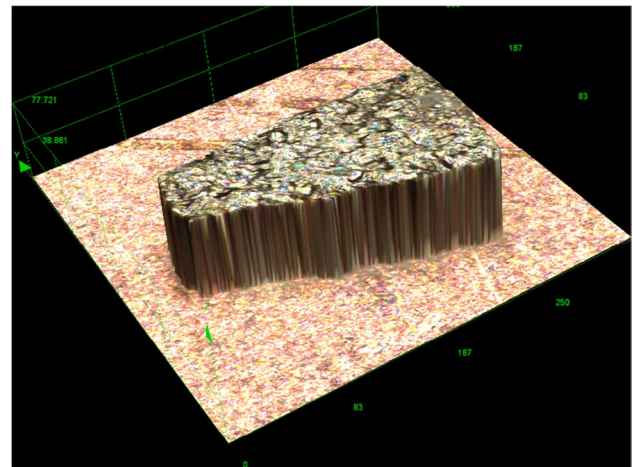

Fig. 8 3D reconstruction of one laser machined segment Sm2Co17 micromagnet

Fig. 8. Inner radius, outer radius, thickness, and angle have been measured using IC measure software and shown in Fig. 9.

Thickness has been determined using two independent methods: 3D imaging reconstruction with the digital microscope, and directly measuring thickness with a lateral view of the micromagnets, as shown in Fig. 10. Micromagnets were manipulated using plastic tweezers to avoid any structural damage.

A summary of the geometric dimensions is given in Table 1. All dimensions are in good agreement with the design and within the targeted range of tolerance described in Fig. 2.

From a structural point of view, microsegment presents good consistency and rigidity. They were manipulated using plastic microtwezeers, gripping and releasing them easily without damage or chips generation during the manipulation. Flatness of top surface has been calculated in 0.005 mm from profile measurements. Perpendicularity of 0.006 has been calculated.
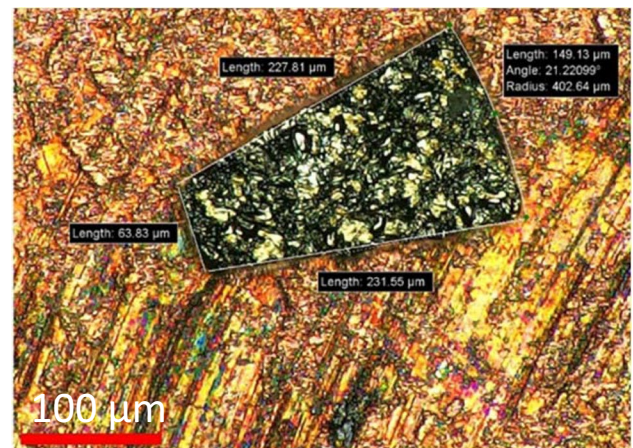

Fig. 9 Top view of a Sm2Co17 micromagnet and geometric characteristics. Scale bar: 100 μm

Fig. 7 Optical microscope images of two segment Sm2Co17 micromagnets. Scale bars: 50 um (left) and 100 um (right)
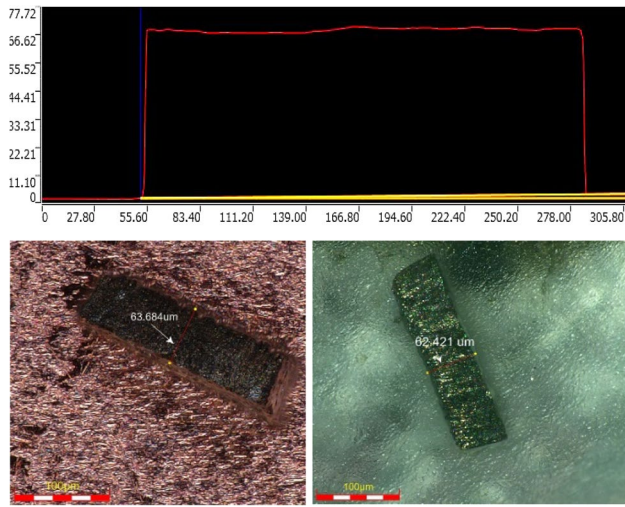
Fig. 10 Thickness measurement: profilometer microscope measurement (top) and side view optical measurement (bottom) for one the segment Sm2Co17 micromagnets. Scale bar (bottom images): 100 μm

Fig. 11 SEM image of the top surface of one of the resulting Sm2Co17 micromagnets. Scale bar: 50 μm

3.2 Surface roughness measurements and analysis

Analysis of the surface roughness has been done from SEM images and from surface roughness measurements obtained through digital microscope profilometer function.

Top surface of the magnet shows typical laser-induced periodic surface structures as shown in Fig. 11. The average surface roughness of this top laser treated surface is Ra = 2.56 μm.

Lateral surface, after cutting, does not show significant melt debris. Cuts are straight and clean. As Sm_2Co_{17} is highly resistant to corrosion and oxidation [49], no accumulation of oxides is expected in this lateral surface. Lateral surface and bottom surface are shown in Fig. 12. Bottom surface is the same of the initial magnet since that side was not processed. This surface was finished by conventional grinding and its average surface roughness has been measured in Ra = 3.13 um.

3.3 Magnetic measurements

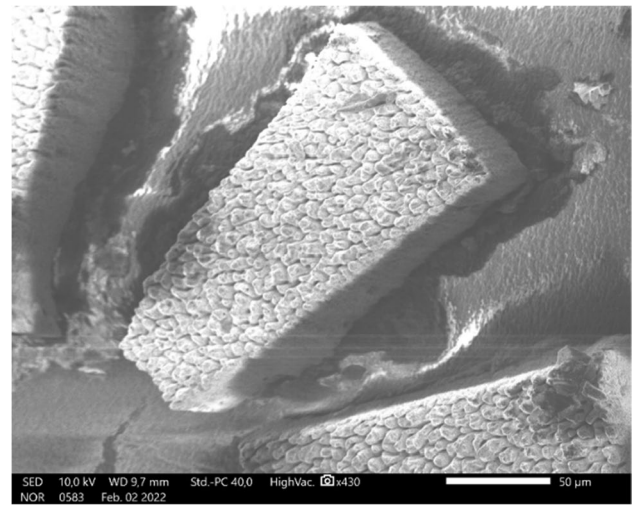Magnetometric studies have been performed for some microsegment magnets to determine if the laser cutting process

generates thermal permanent damage, which would translate into decreased permanent magnet properties.

Microsegment magnets were magnetized in a magnetizer with a solenoid coils fixture. The fixture can generate up to 5.5T of magnetic field in the center of the solenoid. This magnetic field is strong enough to fully magnetize Sm_2Co_{17} Recoma35E magnets. Micromagnets were hold on a support with adhesive tape and magnetized in the axial direction by applying a train of three consecutive 5.5-T pulsed fields.

The measurement of the magnetization level of the segments has been done by two independent methods: direct measurement of the axial magnetic field of the magnetic and BH curve measurement with a vibrating sample magnetometer (VSM).

In the first method, a measurement set up based on a Hall effect microsensor has been prepared for measuring the magnetic field of the microsegments along the axial direction. Distance between hall sensor and magnet top surface has been previously calibrated. Then, a set of magnetic field measurement versus distance has been obtained. Both the positive and negative poles are measured. The position of maximum magnetic field in the horizontal plane is detected. Once the maximum is detected, several measures of magnetic flux density are taken at different high values.

Table 1 Design and measured dimensions. Equipment measurement error ±3 μm

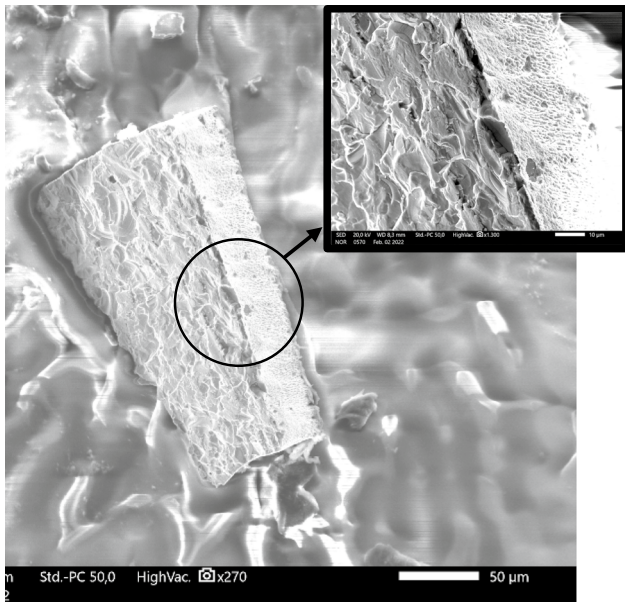|	Thickness (μm)	Inner radius (μm)	Outer radius (μm)	Angle (°)
Target	65	175	400	20
Sample 1	63.372	173.54	402.64	21.22
Sample 2	63.684	176.32	405.78	19.28
Sample 3	62.421	172.34	398.56	20.76
Avg/dev	63.2±0.7	174.1±2	402±3.6	20.4±1

Fig. 12 SEM image showing bottom and lateral surfaces of a Sm2Co17 micromagnet. Inset: zoom image

These measurements have been compared with the values given by simulations done in ANSYS Electronics Maxwell considering the shape of the micromagnet and the Sm_2Co_{17} RECOMA 35E properties. The comparison between measurements and simulation is shown in Fig. 13. The results demonstrate that the magnetic saturation is reached in the magnets, which exhibits magnetic properties close to the original properties of the raw material. The ratio between magnetic field measurement and expected magnetic field is 90% with a deviation of $\pm 10\%$ for the positive pole, while the ratio of the negative pole is $110\% \pm 10\%$. Based on these results, we can state that
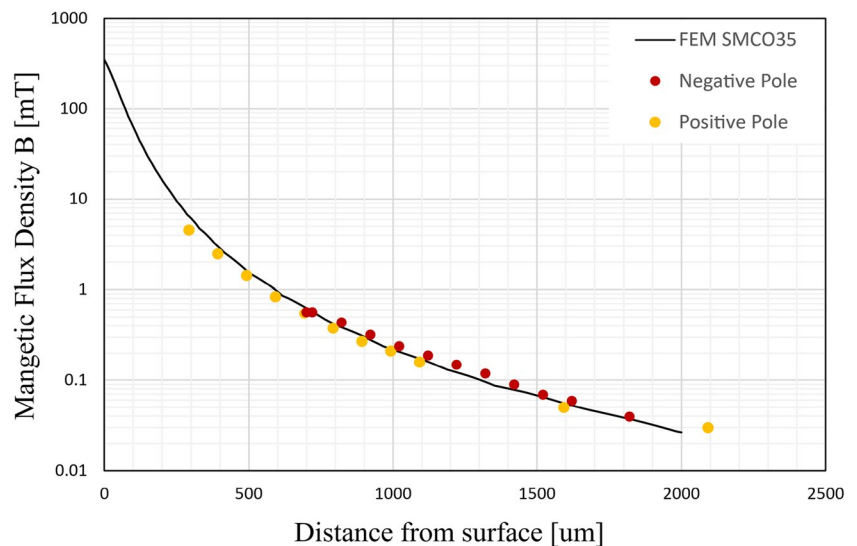
the heat-affected zone, if any, is neglectable as for the magnetic performance refers.

As a second mean of validation, the microsegments were measured in a VSM magnetometer to measure the magnetic properties of the material. The properties of the raw initial Sm2Co17 magnet disk have been also measured for the sake of comparison. The graph of Fig. 14 shows the magnetization curves of one of the microsegments and the raw original disk for comparison. The original disk has a saturation magnetization (Ms) value of 104.8 emu/g and remanent magnetization (Mr) value of 97.0 emu/g. The considered microsegment has a Ms value of 108.4 emu/g and Mr value of 97.2 emu/g. Taking into consideration that the relative error accompanying the magnetization measurement is 5%, the obtained values are approximately the same for both the initial whole magnet and the micromagnet obtained from it. Coercivity values could not be precisely determined due to the limitation in the maximum strength field of the equipment (2.5 T), which prevented to fully demagnetize the samples (Fig. 12), which were saturated before mounting the samples in the VSM. However, coercivity for both samples can be extrapolated to about 26 kOe (Fig. 12) in good agreement with values provided by the manufacturer for Sm_2Co_{17} RECOMA35E. These results support the efficiency of the applied process to fabricate micromagnets with no deterioration of the initial magnetic properties.

4 Conclusions

An ultrashort pulsed laser machining process for precision manufacturing of Sm_2Co_{17} micromagnets is proposed in this work. The laser machining process has a special feature very adequate for micromagnets based on the possibility of cutting microparts submerged in a refrigerant fluid.
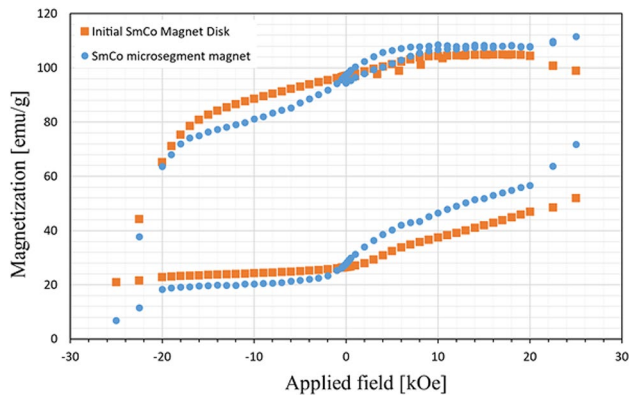
Fig. 13 FEM simulation and measurements of magnetic flux density for microsegment magnet 1 as an example

Fig. 14 Room temperature magnetization measurements of a microsegment and the initial Sm_2Co_{17} disk for comparison

This is especially beneficial for magnets as it drastically reduces the heat effect induced by laser cutting on the hard magnetic materials, which are very sensitive to high temperature (responsible of microstructural damage resulting in detrimental magnetic properties). A complex microsegment shape with around 65 µm in thickness has been fabricated starting from a Sm_2Co_{17} disk that was initially manufactured using classical mechanical means. The dimensions of the permanent magnets reported in this paper make them the smallest sintered Sm_2CO_{17} micromagnets ever fabricated without using costly lithography techniques. Preservation of the magnetic properties after processing has been validated by measuring the magnetic flux density at different distances from the surface and by measurement of BH curves. Therefore, this technique allows the manufacturing of permanent micromagnets for applications like MEMS or microactuators, with 2D-3 complex features in a custom height and shapes from bulk Sm_2Co_{17} magnets.

Author contribution Gabriel Villalba-Alumberos: writing — review and editing, methodology, investigation. Alberto Bollero and Jimena Soler-Morala: funding acquisition, management and conceptualization of research, data curation and writing, investigation. Alexander Kanitz: validation, resources. Jan Hoppius: software, investigation. Ignacio Valiente-Blanco: validation, resources. Efren Diez-Jimenez: validation, writing — original draft.

Declarations

Conflict of interest The authors declare no competing interests.

References

1. Rallabandi V, Taran N, Ionel DM, Boldea IG (2017) Axial-flux PM synchronous machines with air-gap profiling and very high ratio of spoke rotor poles to stator concentrated coils. 2017 IEEE Int Electr Mach Drives Conf IEMDC. IEEE; 2017;1–7

2. Diez-Jimenez E, Rizzo R, Gómez-García MJ, Corral-Abad E (2019) Review of passive electromagnetic devices for vibration damping and isolation. Shock Vib

3. Diez-Jimenez E, Alén-Cordero C, Alcover-Sánchez R, Corral-Abad E (2021) Modelling and test of an integrated magnetic spring-eddy current damper for space applications. Actuators 10:1–18

4. Diez-Jimenez E, Musolino A, Raugi M, Rizzo R, Sani L (2019) A magneto-rheological brake excited by permanent magnets. Appl Comput Electromagn Soc J 34:186–191

5. Diez-Jimenez E, Sanchez-Montero R, Martinez-Muñoz M (2017) Towards miniaturization of magnetic gears: torque performance assessment. Micromachines 9:16. [cited 2018 May 29]. Available from: http://www.mdpi.com/2072-666X/9/1/16

6. Zhao B, Bai Z, Lv H, Yan Z, Du Y, Guo X et al (2023) Self-healing liquid metal magnetic hydrogels for smart feedback sensors and high-performance electromagnetic shielding. Nano-Micro Lett 15:1–14. Springer Science and Business Media B.V [cited 2023 May 4]. Available from: https://link.springer.com/article/10.1007/s40820-023-01043-3

7. Vidal J V., Slabov V, Kholkin AL, dos Santos MPS (2021) Hybrid triboelectric-electromagnetic nanogenerators for mechanical energy harvesting: a review. Nano-Micro Lett 13:1–58. Springer [cited 2023 May 4]. Available from: https://link.springer.com/article/10.1007/s40820-021-00713-4

8. Zhou Q, Ji B, Hu F, Luo J, Zhou B (2021) Magnetized micropillar-enabled wearable sensors for touchless and intelligent information communication. Nano-Micro Lett 13:1–16. Springer Science and Business Media B.V. [cited 2023 May 4]. Available from: https://link.springer.com/article/10.1007/s40820-021-00720-5

9. Vaccumshmeltze: Iron-cobalt alloys

10. Zheng Y, Zhao H, Cai Y, Jurado-Sánchez B, Dong R (2022) Recent advances in one-dimensional micro/nanomotors: fabrication, propulsion and application. Nano Micro Lett 15:1–29. Springer [cited 2023 May 4]. Available from: https://link.springer.com/article/10.1007/s40820-022-00988-1

11. Wang J, Dong R, Wu H, Cai Y, Ren B (2019) A review on artificial micro/nanomotors for cancer-targeted delivery, diagnosis, and therapy. Nano-Micro Lett 12:1–19. Springer [cited 2023 May 4]. Available from: https://link.springer.com/article/10.1007/s40820-019-0350-5

12. Qin K, Chen C, Pu X, Tang Q, He W, Liu Y et al (2021) Magnetic array assisted triboelectric nanogenerator sensor for real-time gesture interaction. Nano-Micro Lett 13:1–9. Springer Science and Business Media B.V

13. Choi S, Kim SH, Yoon YK, Allen MG (2006) A magnetically excited and sensed MEMS-based resonant compass. IEEE Trans Magn 42:3506–3508

14. Jackson N, Pedrosa FJ, Bollero A, Mathewson A, Olszewski OZ (2016) Integration of thick-film permanent magnets for MEMS applications. J Microelectromech Syst 25:716–724

15. Lu H, Zhu J, Guo Y (2005) Development of a slotless tubular linear interior permanent magnet micro motor for robotic applications. INTERMAG ASIA 2005 Dig IEEE Int Magn Conf 41:105

16. Yufeng S, Wenyuan C, Feng C, Weiping Z (2006) Electro-magnetically actuated valveless micropump with two flexible diaphragms. Int J Adv Manuf Technol 30:215–220

17. Hagiwara M, Kawahara T, Feng L, Yamanishi Y, Arai F (2011) On-chip dual-arm microrobot driven by permanent magnets for

high speed cell enucleation. Proc IEEE Int Conf Micro Electro Mech Syst. IEEE; 189–92

18. Liu Z, Nakamura T (2006) Realization of wire-in-hole operation with a two-finger precision manipulator. Int J Adv Manuf Technol 28:1230–1236

19. Fratzl M, Delshadi S, Devillers T, Bruckert F, Cugat O, Dempsey NM et al (2018) Magnetophoretic induced convective capture of highly diffusive superparamagnetic nanoparticles. Soft Matter 14:2671–2681

20. Munoz F, Alici G, Li W, Sitti M (2016) Size optimization of a magnetic system for drug delivery with capsule robots. IEEE Trans Magn. IEEE 52

21. Villalba-Alumbreros G, Moron-Alguacil C, Fernandez-Munoz M, Valiente-Blanco I, Diez-Jimenez E (2022) Scale effects on performance of BLDC micromotors for internal biomedical applications: a finite element analysis. J Med Device :16. American Society of Mechanical Engineers Digital Collection [cited 2022 Jul 5]. Available from: https://asmedigitalcollection.asme.org/medicaldevices/artic le/16/3/031011/1140703/Scale-Effects-on-Performance-of-BLDC-Micromotors

22. Martínez Rojas JA, Fernández JL, Montero RS, Espí PLL, Diez-Jimenez E (2021) Model-based systems engineering applied to trade-off analysis of wireless power transfer technologies for implanted biomedical microdevices. Sensors 21

23. Martinez-Muñoz M, Diez-Jimenez E, Villalba-Alumbreros GV, Michalowski M, Lastra-Sedano A (2019) Geometrical dependence in fixtures for 2D multipole micromagnets magnetization pattering. Appl Comput Electromagn Soc J 34

24. Bodduluri MT, Lisec T, Blohm L, Lofink F, Wagner B (2019) High-performance integrated hard magnets for MEMS applications. MikroSystemTechnik Kongress 2019 - Mikroelektron MEMS-MOEMS Syst - Saulen der Digit und Kunstl Intelligenz, Proc. 150–3

25. Villalba-Alumbreros G, Lopez-Camara E, Martínez-Gómez J, Cobreces S, Valiente-Blanco I, Diez-Jimenez E (2023) Experimental study of micromilling process and deburring electropolishing process on FeCo-based soft magnetic alloys. Int J Adv Manuf Technol :3235–48. Springer London

26. Diez-Jimenez E, Valiente-Blanco I, Villalba-Alumbreros G, Fernandez-Munoz M, Lopez-Pascual D, Lastra-Sedano A et al (2022) Multilayered microcoils for microactuators and characterization of their operational limits in body-like environments. IEEE/ASME Trans Mechatronics, 1–6

27. Villalba-alumbreros G, Fernandez-munoz M, Lopez-pascual D, Valiente I, Lastra-sedano A, Díez-Jimenez E (2022) Desarrollo de una máquina bobinadora semiautomática para la microfabricación de bobinados, antenas y solenoides micrométricos, pp 22–4

28. ListenInc (2008) Permanent Magnets For MEMS. 18:1255–66

29. Timoshkov IV, Khanko AV, Kurmashev VI, Grapov DV, Kastevich AA, Govor GA et al (2019) Applications of UV-LIGA and grayscale lithography for display technologies. Dokl BGUIR 7:81–87

30. Khosla A, Kassegne S (2015) Fabrication of NdFeB-based permanent rare-earth micromagnets by novel hybrid micromolding process. Microsyst Technol 21:2315–2320

31. Jiang Y, Masaoka S, Uehara M, Fujita T, Higuchi K, Maenaka K (2011) Micro-structuring of thick NdFeB films using high-power plasma etching for magnetic MEMS application. J Micromech Microeng 21

32. Keller FO, Haettel R, Devillers T, Dempsey NM (2022) Batch fabrication of 50 μm-thick anisotropic Nd-Fe-B micro-magnets. IEEE Trans Magn 58

33. Nakamura H, Hirota K, Minowa T, Honshima M (2005) Magnetic properties of extremely small Nd-Fe-B sintered magnet. INTERMAG ASIA 2005 Dig IEEE Int Magn Conf 41:476

34. Knowles MRH, Rutterford G, Karnakis D, Ferguson A (2007) Micro-machining of metals, ceramics and polymers using nanosecond lasers. Int J Adv Manuf Technol 33:95–102

35. Putzer M, Ackerl N, Wegener K (2021) Geometry assessment of ultra-short pulsed laser drilled micro-holes. Int J Adv Manuf Technol. The International Journal of Advanced Manufacturing Technology 117:2445–2452

36. Zheng HY, Liu H, Wan S, Lim GC, Nikumb S, Chen Q (2006) Ultrashort pulse laser micromachined microchannels and their application in an optical switch. Int J Adv Manuf Technol 27:925–929

37. Geng Z, Tong Z, Huang G, Zhong W, Cui C, Xu X et al (2022) Micro-grooving of brittle materials using textured diamond grinding wheels shaped by an integrated nanosecond laser system. Int J Adv Manuf Technol. Springer London 119:5389–5399

38. Park CK, Farson DF (2016) Precise machining of disk shapes from thick metal substrates by femtosecond laser ablation. Int J Adv Manuf Technol 83:2049–2056

39. Peterson BA (2016) Geometrically-complex magnetic field distributions enabled by bulk, laser-micromachined permanent magnets at the submillimeter scale [Internet]. Publicly Access. Penn Diss. Available from: http://ezproxy.lib.ryerson.ca/login?url=https://search.proquest.com/docview/1859672253?accountid=13631%0Ahttp://sfx.scholarsportal.info/ryerson??url_ver=Z39.88-2004&rft_val_fmt=info:ofi/fmt:kev:mtx:dissertation&genre=dissertations+%26+theses&sid=ProQ:ProQ

40. Peterson BA, Herrault F, Oniku OD, Kaufman ZA, Arnold DP, Allen MG (2012) Assessment of laser-induced damage in laser-micromachined rare-earth permanent magnets. IEEE Trans Magn 48:3606–3609

41. Marimuthu S, Smith B (2021) Water-jet guided laser drilling of thermal barrier coated aerospace alloy. Int J Adv Manuf Technol 113:177–191

42. Zhang Q, Sun SF, Zhang FY, Wang J, Lv QQ, Shao Y et al (2020) A study on film hole drilling of IN718 superalloy via laser machining combined with high temperature chemical etching. Int J Adv Manuf Technol 106:155–162

43. Kanitz A, Hoppius JS, Fiebrandt M, Awakowicz P, Esen C, Ostendorf A et al (2017) Impact of liquid environment on femtosecond laser ablation. Appl Phys A Mater Sci Process 123:1–7. Springer Berlin Heidelberg

44. Maack P, Kanitz A, Hoppius J, Köhler J, Esen C, Ostendorf A (2022) Surface modification of silicon by femtosecond laser ablation in liquid. In: Watanabe A, Kling R, editors. Laser-based micro- nanoprocessing XVI. SPIE, p. 119890L. https://doi.org/10.1117/12.2608708

45. Kanitz A, Kalus MR, Gurevich EL, Ostendorf A, Barcikowski S, Amans D (2019) Review on experimental and theoretical investigations of the early stage, femtoseconds to microseconds processes during laser ablation in liquid-phase for the synthesis of colloidal nanoparticles. Plasma Sources Sci Technol 28

46. Hoppius JS, Maragkaki S, Kanitz A, Gregorčič P, Gurevich EL (2019) Optimization of femtosecond laser processing in liquids. Appl Surf Sci 467–468:255–60. Elsevier. https://doi.org/10.1016/j.apsusc.2018.10.121

47. Menéndez-Manjón A, Wagener P, Barcikowski S (2011) Transfer-matrix method for efficient ablation by pulsed laser ablation and nanoparticle generation in liquids. J Phys Chem C 115:5108–14. [cited 2023 Aug 22]. Available from: https://pubs.acs.org/sharingguidelines

48. Shih CY, Streubel R, Heberle J, Letzel A, Shugaev MV, Wu C et al (2018) Two mechanisms of nanoparticle generation in picosecond laser ablation in liquids: the origin of the bimodal size distribution. Nanoscale 10:6900–10. The Royal Society of Chemistry; [cited 2023 Aug 22]. Available from: https://pubs.rsc.org/en/content/articlehtml/2018/nr/c7nr08614h

49. Kardelky S, Gebert A, Gutfleisch O, Hoffmann V, Schultz L (2005) Prediction of the oxidation behaviour of Sm-Co-based magnets. J Magn Magn Mater 290-291 PA:1226–9